JOURNAL OF OPTOELECTRONICS AND ADVANCED MATERIALS Vol. 12, No. 3, March 2010, p. 518 - 522

Influence of etching and surface functionalization on the optical property of luminescing phosphorus doped silicon nanoparticles

A. GUPTA[a*], C. SCHULZ[a,b], H. WIGGERS[a,b*]
[a]*Institute for Combustion and Gasdynamics (IVG), University of Duisburg-Essen, Duisburg, Germany*
[b]*Center for Nanointegration Duisburg-Essen (CeNIDE), University of Duisburg-Essen, Duisburg, Germany*

In this study, we investigated the photoluminescence (PL) behavior of phosphorus-doped silicon nanoparticles (P-doped Si-NPs) after etching and surface functionalization processes. Si-NPs were synthesized in a low-pressure microwave plasma reactor via pyrolysis of silane (SiH_4). Doping of phosphorus into Si-NPs was carried out by injection of phosphine during the gas-phase synthesis of Si-NPs. The emission of P-doped Si-NPs was tuned from red to blue by etching them in a mixture of hydrofluoric acid (HF) and nitric acid (HNO_3) for different times. Air oxidation of freshly etched NPs causes a blue shift in the emission spectra and decreasing intensity. Surface functionalization of etched NPs also alters their emission wavelength; however, functionalized NPs show stable bright emission for several months.

(Received June 21, 2009; accepted October 13, 2009)

Keywords: Doped silicon nanoparticles, Surface functionalization, Photoluminescence, FTIR spectroscopy

1. Introduction

The continuous trend in electronics and optoelectronics to reduce device sizes down to nanometer scales has led to wide ranging scientific interest in nanoparticles of all kinds of materials during the last few years. Especially, the discovery of visible photoluminescence (PL) from silicon nanoparticles (Si-NPs) by Canham *[1]* has attracted a great deal of attention as it renews the hope to integrate light-emitting devices based on silicon with the well-established microelectronics technology. As a prerequisite, the combination of microelectronics and nanoparticles requires functional structures that are based on p- and n-doped materials. The promise of nanomaterials as a technological material, for applications including wavelength tunable lasers *[2]*, bioimaging *[3]*, and solar cells *[4]*, may ultimately depend on tailoring their behavior through doping. For this reason, researchers have begun dope films containing Si-NPs as well as freestanding nanoparticles and explored how dopants can influence semiconducting nanomaterials. For example, doping of phosphorus (P) atoms into Si-NPs has been achieved by co-sputtering of silicon and phosphosilicate glasses *[5]*, by pulse injection of PH_3 during the formation of Si-NPs from SiH_4 on thermally grown SiO_2 *[6]*, and by non-thermal plasma synthesis by use of diborane and phosphine *[7]*. Doping of boron (B) into Si-NPs is reported to deteriorate their PL properties. The quenching of PL intensity was observed with increasing doping level of B atoms into Si-NPs due to Auger recombination of excitons *[5]*. Whereas the P doping into Si-NPs enhances their PL intensity by quenching the defect related recombination, however, the increase in PL intensity was observed up to a certain concentration of P atoms and thereafter it decreases as interavalley transition of free electrons generated by P doping appears *[5]*. Stegner et al. *[8]* showed that the electronic transport in compacted Si-NPs film is significantly enhanced with P doping. The increase in the P doping level can increase the conductivity and decrease the temperature dependence change in conductivity.

Thus, the properties of P-doped Si-NPs are very sensitive to the doping level and well studied in the past. The future exploitation of P-doped Si-NPs depends on further understanding their behavior with change in composition, size and surface chemistry. In this contribution, microwave plasma synthesis of freestanding P-doped Si-NPs is presented. The optical behavior of P-doped Si-NPs is studied by varying their size. Furthermore, the influence of doping, surface oxidation and surface functionalization on the optical properties of P-doped Si-NPs is examined. Therefore, our approach opens a new way to synthesize P-doped Si-NPs and gives a new insight to understand their optical properties.

2 Experimental

A microwave plasma reactor was used to synthesize P-doped Si-NPs. A sketch of the setup is schematically depicted in Figure 1. In this synthesis approach, the precursor (10 % SiH_4 in Ar) and dilute gases (Ar and H_2) are injected into the reaction chamber together with dopant gas (0.1 % PH_3 in Ar). The microwave energy is used to ignite the plasma and NPs are formed by nucleation and growth processes. The microwave generator was driven at

2.45 GHz frequency and 1200 W power. The precursor and dopant concentrations were adjusted at 3000 ppm and 30 ppm, respectively. The total gas pressure in the reaction chamber was kept at about 5 kPa.

The surface etching of P-doped Si-NPs was carried out in a glove box by adding HF (50 wt%) and HNO_3 (70 wt%) (10/1 v/v) mixture into their dispersion in methanol. The solution was then stirred for 10-20 minutes and then the particles were collected onto the filter paper. Thereafter, the particles were washed first with HF acid to increase the hydrogen coverage on the surface and then with methanol to remove the traces of HF acid. In semiconductor industry, the doping concentration is defined by the number of dopant atoms per cubic centimeter. Therefore in our experiments, the P doping level can be estimated by atomic density of bulk Si multiplied by the fraction of phosphine in the total flow of precursor gases during synthesis. The calculated doping concentration of P atoms into the Si-NPs was approximately $5 \cdot 10^{20}$ cm^{-3}. As secondary ion mass spectroscopy (SIMS) investigations on the P-doped samples reveal that about 95 % of the phosphorus is located in the outer sphere of the Si nanocrystals, the remaining concentration of P in the etched particles is about $2.5 \cdot 10^{19}$ cm^{-3} *[9]*. The surface functionalization of P-doped Si-NPs was accomplished by a photoinitiated hydrosilylation process *[10]*. In order to do that, the freshly etched particles from the filter paper were dispersed into the alkene (1-dodecene was used in this experiment) via ultrasonic agitation and then the solution was exposed to the UV light (λ = 253.7 nm) for 10 h.

The surface chemistry of Si NPs was investigated by Fourier transform infrared (FTIR) spectroscopy in diffuse reflectance mode using a Bruker IFS66v/S spectrometer. A Perkin-Elmer LS 50 Fluorescence spectrometer was used for photoluminescence (PL) measurements. All emission spectra were recorded at room temperature using an excitation wavelength of 350 nm. Transmission electron microscopy (TEM) investigation was performed using Philips CM-20 at an operating voltage 200 kV. All photographs of luminescing Si-NPs were taken by exposing them to UV light (λ = 366 nm).

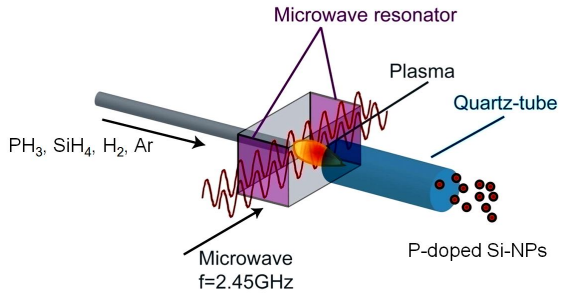

Fig. 1. Schematic of the experimental setup for the synthesis of P-doped Si-NPs in a microwave plasma reactor.

3 Results and discussions

Representative TEM images of as-prepared P-doped Si-NPs are shown in Figure 2. These nanoparticles are highly agglomerated, almost spherical in shape and highly crystalline in nature. The High Resolution TEM (HR-TEM) image (inset, Fig. 2a) clearly shows the lattice fringes of these NPs. An amorphous oxide shell is formed around the crystalline core due to the natural oxidation of these NPs upon air exposure (inset, Fig. 2a). The particles show lognormal size distribution with an average diameter (d_p) of 17 nm and a geometric standard deviation (σ_g) of 1.5 (Fig. 2b).

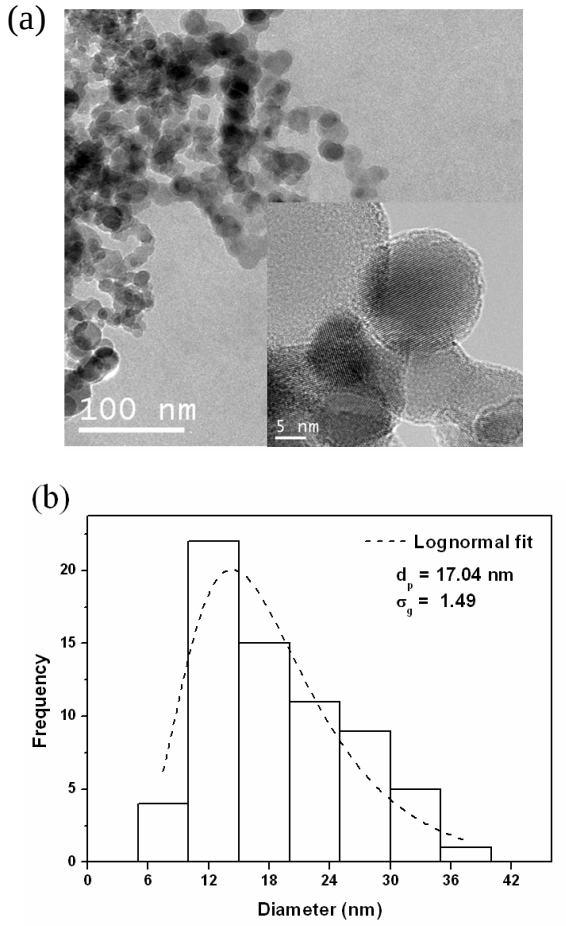

Fig. 2. a) Bright field TEM image of as-prepared nanoparticles. The inset is a HR-TEM image showing an amorphous oxide layer on the circumference of the crystalline silicon core. b) Histogram and log-normal fit of the particle size distribution of as-prepared sample.

Fig. 3 shows the change in PL emission spectrum of P-doped Si-NPs during the etching process and the pictures of their dispersion in chloroform under UV illumination. The as-prepared particles do not exhibit any visible PL neither as a dry powder nor after dispersion in a solvent due to their big size. However, after few minutes of etching with HF and HNO_3 mixture as described above,

the particles start to show PL in the visible. During the etching process, the surface oxides are dissolved and the size of NPs decreases by simultaneous oxidation (by HNO_3) and dissolution of oxides (by HF). The increase in etching time causes the continuous blue shift in their PL spectra from red to green, which is supposed to originate from the decrease in particle size *[11-13]*. We experienced that the blue emission from P-doped Si-NPs is very difficult to obtain from this etching procedure. The origin of blue emission is still unclear to us as we observed the blue emission from P-doped Si-NPs only once at a random etching time and it was never obtained by increasing etching time after the green emission. We also observed the similar behavior in case of undoped Si-NPs *[11]*.

As can be seen from Figure 3, the PL spectrum of Si-NPs with the luminescence maximum at 749 nm is quite noisy compared to the other spectra. This is attributed to its low intensity compared to the other spectra and it also shows an additional signal around 650 nm. The same feature was observed from Svrcek et al. *[14]* for silicon nanocrystals prepared by electrochemical etching. They attributed the signal around 740 nm to the existence of surface states and defects at the surface of the Si-NPs. These defects are preferentially found in P-doped silicon.

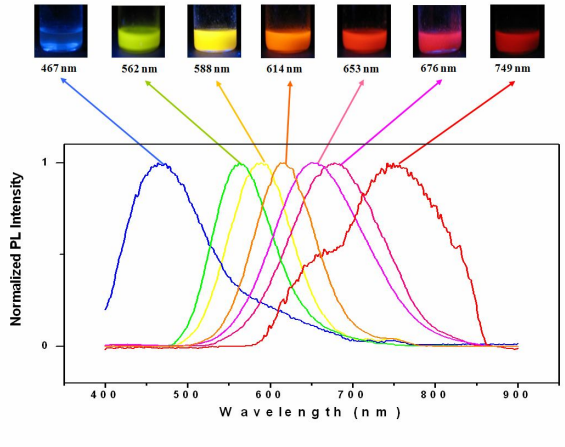

Fig. 3. Normalized photoluminescence spectra of P-doped Si-NPs produced at different etching time and their corresponding dispersion in chloroform under UV illumination.

Despite the fact that we synthesized etched nanoparticles with a quite high phosphorus concentration of about $2.5 \cdot 10^{19}$ cm^{-3}, we did not observe an increase in PL intensity as discussed in *[5]* compared to undoped nanocrystals *[11-13]*. According to Delerue et al. *[12]*, the nanocrystal size can be calculated from the emission spectra via

$$E_g(\mathrm{eV})(d) = E_0(\mathrm{eV}) + \frac{3.73}{d(\mathrm{nm})^{1.39}}$$

Applying this equation, the diameter of nanocrystals luminescing between 750 nm and 560 nm decreases from 4.0 nm to 2.4 nm and the associated number of silicon atoms/crystal decreases from 2000 to 500. This means, that the bigger crystals statistically contain only 1 phosphorus atom per particle. Therefore we do not expect a strong influence from the dopant on the PL properties but a much higher influence from the particle surface, as for particles with a size of 4.0 nm about 30 % of the atoms are located at the particle surface.

The FTIR spectra of as-prepared and freshly etched P-doped Si-NPs are presented in Figure 4. The spectrum of as-prepared sample contains characteristic vibration modes of silicon oxide with different stoichiometric composition. These are the signatures from $HSi\text{-}O_3$ stretching mode at 2260 cm^{-1} *[15]*, $HSi\text{-}O_2Si$ stretching mode at 2200 cm^{-1} *[15]*, and Si-O-Si asymmetric stretching mode at 1180 cm^{-1} and at 1068 cm^{-1} *[16]*. The oxides are formed due to exposure of NPs in air. A small peak of $Si\text{-}H_n$ (n = 1–3) stretching mode around 2100 cm^{-1} *[17]* is also observed in the spectrum of as-prepared sample. The FTIR spectrum of etched Si-NPs clearly shows the increase in $Si\text{-}H_n$ stretching vibration mode along with the complete disappearance of $HSi\text{-}O_2Si$, $HSi\text{-}O_3$ and Si-O-Si vibration signals. This indicates that the etching process completely removes surface oxides and also terminates the silicon surface with hydrogen.

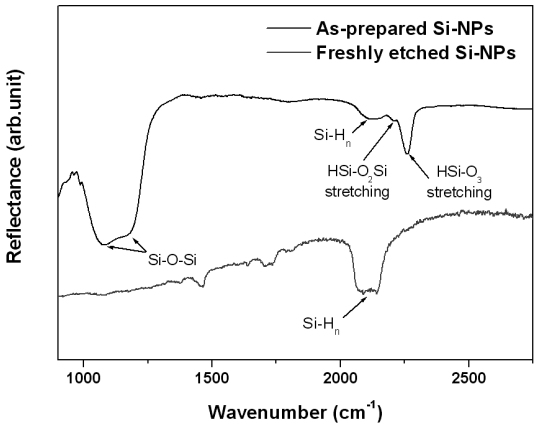

Fig. 4. FTIR spectra of as-prepared and freshly etched P-doped Si-NPs.

We find that the PL of etched P-doped Si-NPs is unstable in air. As an example, we show the PL emission spectra of green emitting NPs as a function of air exposure time (Fig. 5). As the air exposure time increases, the PL peak of green emitting etched NPs at 580 nm continuously shifts towards lower wavelength (blue shift) with decreasing PL intensity. The underlying mechanism is the re-oxidation of freshly etched P-doped Si-NPs in air. The oxidation of etched NPs decreases the size of crystalline silicon core and therefore causes the blue shift according to quantum confinement effect *[18]*. The oxidation of etched Si-NPs is associated with the introduction of defects (such as vacancies and dangling bonds) that lead to non-radiative recombination of excitons at the interface of crystalline core and oxide shell *[19]*. Therefore, the

decrease in PL intensity of etched NPs can be directly correlated to the ingression of defect centers due to their surface oxidation.

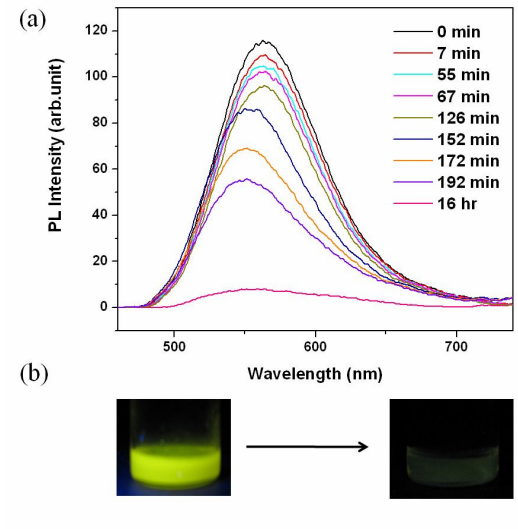

Fig. 5. a) PL spectra of green emitting etched P-doped Si-NPs as a function of air-exposure time. b) Picture of etched NPs under UV illumination: freshly etched (left) and after 1 days of air exposure (right).

In order to stabilize etched P-doped Si-NPs against oxidation, we coated their surface with organic molecules. For this purpose, the surface of NPs is chemically bond to dodecyl molecules via a photoinitiated alkylation process (see experimental section for details). After this functionalization process, the functionalized NPs were separated from 1-dodecene solution by centrifugation, then washed with methanol and dried in vacuum. Figure 6a shows the FTIR spectra of P-doped Si-NPs after their surface grafting with dodecyl molecules. The CH vibration peaks ($C\text{-}CH_3$ asymmetric stretching at 2958 cm^{-1}, $C\text{-}CH_2$ asymmetric stretching at 2925 cm^{-1} and $C\text{-}CH_2$ symmetric stretching 2856 cm^{-1}) *[20]* originates from the dodecyl molecules attached on their surface. Additionally, peaks from SiH_n vibration modes are still present in the spectrum, which consists of SiH_3 (2134 cm^{-1}), SiH_2 (2102 cm^{-1}) and SiH (2082 cm^{-1}) stretching vibrations *[17]*. The characteristic peaks of dodecyl molecules along with the remaining hydrogen terminated vibration modes indicate the partial functionalization of silicon surface. The initially attached alkyl groups on the silicon surface provide an increasing steric hindrance for further attachment of organic molecules, which results in incomplete coverage of the silicon surface. In the spectrum of functionalized sample, a small signature of Si-O-Si vibration mode at 1070 cm^{-1} is also observed. This indicates that the surface of silicon nanoparticles is slightly oxidized during the functionalization due to the presence of some traces of oxygen in the solution.

We observed that freshly etched NPs show a change in their emission wavelength after the surface functionalization process. As shown in Figure 6b, the freshly etched green emitting P-doped Si-NPs show red shift after their surface functionalization and emit in yellow-orange regime. Functionalization process changes the chemistry of surface from hydrogen terminated to alkyl terminated. The change in surface chemistry is reported to decrease the HOMO-LUMO band gap of small silicon NPs *[11, 13, 21]* and some recent reports discuss the leakage of the quantum-confined wavefunction out of the silicon nanocrystals *[22, 23]*. Therefore, the red shift in the PL spectrum of initially green emitting NPs after surface functionalization is expected to originate due to decrease in the optical band gap and some leakage of the wavefunction to the surrounding shell. The remaining number of Si-H bonds on functionalized silicon surface may react with oxygen and form silicon oxides *[24]*, however, the oxidation of functionalized NPs is very slow compared to etched samples as the organic layer on silicon surface provides steric hindrance to the diffusion of oxygen towards the silicon surface and therefore offers long term PL stability. These results show that the surface functionalization process does not stabilize the original emission, however, the emission of functionalized NPs was found be stable for months (visible inspection).

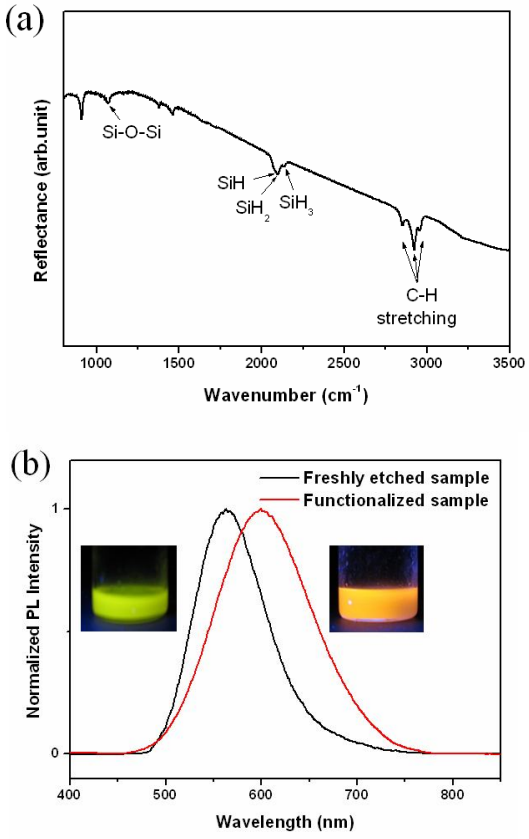

Fig. 6. FTIR spectra of P-doped Si-NPs after their surface functionalization with 1-dodecene. b) Normalized PL spectra of freshly etched and functionalized sample. The sample photographs of etched sample (left) and functionalized sample (right) under UV illumination are also shown.

4. Conclusions

Authors successfully synthesized highly crystalline P-doped Si-NPs from gas phase microwave plasma reactor. The PL of P-doped Si-NPs was tuned across the visible spectrum and we did not observe any increase in the PL intensity of Si-NPs due to phosphorus doping. We find that the air exposure of etched NPs results in a blue shift in the spectrum with decreased intensity. The surface passivation of etched P-doped Si-NPs also causes a shift in their emission spectrum but functionalized particles show long term PL stability in air.

Acknowledgements

Financial support of the German Research Foundation (DFG) through the Research Training Group 1240 (GRK 1240 Nanotronics – Photovoltaik und Optoelektronik aus Nanopartikeln) is greatly acknowledged. The authors are grateful to Marina Spasova for her support with HRTEM measurements.

References

[1] L. T. Canham, Appl. Phys. Lett. **57**, 1046 1990
[2] V. I. Klimov, S. A. Ivanov, J. Nanda, M. Achermann, I. Bezel, J. A. McGuire, A. Piryatinski, Mat. Res. Soc. Symp. Proc. **447**, 441 **(**2007).
[3] X. Michalet, F. F. Pinaud, L. A. Bentolila, J. M. Tsay, S. Doose, J. J. Li, G. Sundaresan, A. M. Wu, S. S. Gambhir, S. Weiss, Science, **307**, 538 (2005).
[4] I. Gur, N. A. Fromer, M. L. Geier, A. P. Alivisatos, Science **310**, 462 (2005).
[5] M. Fujii, A. Mimura, S. Hayashi, D. Kovalev, F. Koch, Mat. Res. Soc. Symp. Proc. **638**, F9.2.1 (2001)
[6] K. Makihara, J. Xu, M. Ikeda, H. Murakami, S. Higashi, S. Miyazaki, Thin Solid Films **508**, 186 (2006).
[7] X. D. Pi, R. Gresback, R. W. Liptak, S. A. Campbell, U. Kortshagen, Appl. Phys. Lett., **92**, 123102 (2008).
[8] A. R. Stegner, R. N. Pereira, K. Klein, R. Lechner, R. Dietmueller, M. S. Brandt, M. Stutzmann, H. Wiggers, Phys. Rev. Lett. **100**, 026803 (2008).
[9] A. R. Stegner, R. N. Pereira, R. Lechner, K. Klein, H. Wiggers, M. Stutzmann, M. S. Brandt, Phys. Rev. B, **80**(16),165326 (2009).
[10] X. Li, Y. He, M. T. Swihart, Langmuir, **20**, 4720 (2004).
[11] A. Gupta, F. Erogbogbo, M. T. Swihart, H. Wiggers, Mat. Res. Soc. Symp. Proc., 1145-MM10-04 (2009).
[12] C. Delerue, G. Allan, M. Lannoo, Phys. Rev. B, **48**, 11024 (1993).
[13] A. Gupta, M. T. Swihart, H. Wiggers, Adv. Funct. Mater., **19**, 696 (2009).
[14] V. Svrcek, H. Fujiwara, M. Kondo, Sol. Energy Mater. Sol. Cells, **93**, 774 (2009).
[15] D. V. Tsu, G. Lucovsky, B. N. Davidson, Phys. Rev. B **40**, 1795 **(**1989).
[16] G. J. Kluth, M. Roya, J. Appl. Phys., **80**, 5408 (1996).
[17] D. C. Marra, E. A. Edelberg, R. L. Naone, E. S. Aydil, J. Vac. Sci. Technol. A, **16**, 3199 (1998).
[18] M. V. Wolkin, J. Jorne, P. M. Fauchet, G. Allan, C. Delerue, Phys. Rev. Lett., **82**, 197 **(**1999)
[19] X. D. Pi, L. Mangolini, S. A. Campbell, U. Kortshagen, Phy. Rev. B, **75**, 085423 (2007).
[20] The Sadtler Handbook of Infrared Spectra, (W. Simons, Ed.). Heyden & Son, Philadelphia, Pa. 1978.
[21] F. A. Reboredo, G. Galli, J. Phys. Chem. B **109**, 1072 (2005).
[22] S. Godefroo, M. Hayne, M. Jivanescu, A. Stesmans, M. Zacharias, O. I. Lebedev, G. Van Tendeloo, V. V. Moshchalkov, Nat. Nano, **3**, 174 (2008).
[23] A. Zimina, S. Eisebitt, W. Eberhardt, J. Heitmann, M. Zacharias, Appl. Phys. Lett., **88**, 163103 (2006).
[24] A. Gupta, H. Wiggers, Physica E, **41**, 1010 (2009).

*Corresponding author: anoop.gupta@uni-due.de
hartmut.wiggers@uni-due.de